Int. J. Multiphase Flow Vol. 15, No. 6, pp. 965–975, 1989
Printed in Great Britain.

0301-9322/89 $3.00 + 0.00

PHASE SEPARATION IN IMPACTING WYES AND TEES

S. T. HWANG,† H. M. SOLIMAN‡ and R. T. LAHEY JR
Department of Nuclear Engineering and Engineering Physics, Rensselaer Polytechnic Institute, Troy, NY 12180-3590, U.S.A.

(*Received* 6 *June* 1988; *in revised form* 15 *March* 1989)

Abstract—An experimental and analytical study of phase separation for impacting two-phase flows in branching conduits has been performed. The resulting analytical model is applicable to impacting flows in wyes and tees for various inlet flow regimes. This model is based on a dividing-streamline concept, and it assumes that there is a "zone of influence" for each of the two phases which is bounded by the conduit wall and the dividing streamlines. Good agreement was obtained between model predictions and the experimental results from this study and others.

Key Words: impacting flows, two-phase, wyes, tees

1. INTRODUCTION

Impacting junctions are defined as those in which the incoming flow (side 1) is split among two coaxial outlet branches (sides 2 and 3). The angle between sides 1 and 3, denoted by θ, is different from 90° for impacting wyes but equal to 90° for the special case of impacting tees. Very little prior work has been done on the problem of phase separation for impacting two-phase flow in branching conduits, however flows of this type are often encountered in practice. For example, the enhancement of petroleum recovery using wet steam injection involves impacting two-phase flows.

Hong (1978) conducted phase separation experiments in relatively small impacting tees (9.525 mm i.d.) He reported equal phase distribution over a wide range of system operating conditions and extraction ratios ($0.15 \leqslant W_3/W_1 \leqslant 0.85$), where W_1 and W_3 are the mass flow rates through sides 1 and 3, respectively.

More recently, Azzopardi *et al.* (1987) reported annular flow phase separation data from an experiment which used an equal-sided impacting tee (32 mm i.d.). The observed data trends were quite different from those of Hong (1978), but were very similar to those of the experiment reported on herein. The reason for this discrepancy is not clear, however, the Weber number, which is a measure of the importance of surface tension, was several orders of magnitude smaller in Hong's experiment than the experiments of Azzopardi *et al.* and ours. Moreover, the axial inertia of the two-phase flow streams exiting the various branches was much smaller in Hong's experiment. It is suspected that Hong's data were influenced by the hydrostatic head of the fluid in the lines leading to the phase separators and by surface tension effects. If these suspicions are correct, then Hong's data should be considered inapplicable to most cases of practical concern.

In the analysis of phase separation in conduits having two outlet branches there are numerous variables which can be considered, however, for steady-state conditions they can be reduced to: the flow rates, W_i ($i = 1, 2$, and 3), the flow qualities, x_i ($i = 1, 2$ and 3) and the pressure changes across the junction, Δp_{13_j} and Δp_{12_j}. Thus we have eight variables. Of these eight, we may specify any three independent variables (e.g. W_1, x_1 and Δp_{13_j}, or x_1, Δp_{13_j} and Δp_{12_j}). We must then be able to solve for the remaining five variables.

The continuity equation for the mixture and the vapor phase, and the mixture momentum equation for both branches provide four independent equations (Saba & Lahey 1984). Specification of the "fifth equation" is not as obvious. Before discussing the derivation of the appropriate relationship let us consider the experiments which have provided some understanding of the phenomena as well as the data needed to assess phase separation models.

†‡Present addresses: †Korea Advanced Energy Research Institute, P.O. Box 7, Daeduk-Danji, Chungnam, Korea; ‡Department of Mechanical Engineering, University of Manitoba, Winnipeg, Manitoba R3T 2N2, Canada.

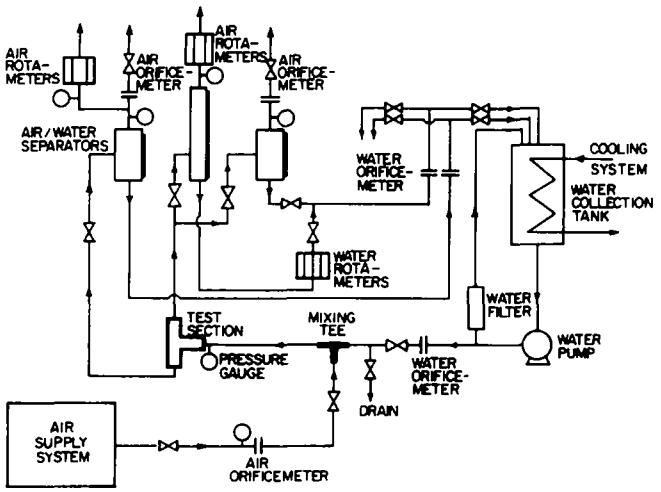

Figure 1. Air–water loop.

2. EXPERIMENTAL RESULTS

The test facility used for the phase separation experiments is shown in figure 1. It consisted of a tee or wye test section, air and water loops and the related instrumentation and computer-based data acquisition system. A hydrodynamic developing length in excess of $50\,L/D$ was placed upstream of the test section. The instrumentation consisted of calibrated orifice flow meters and rotameters, several differential pressure transducers (i.e. Δp cells) and the associated lines and tubing. Mass flow rates of air and water were measured individually at the three sides of the junction and a mass balance on each phase indicated better than 5% accuracy.

Phase separation experiments for impacting flows were performed for the test section configurations shown in figure 2. All the phase separation data were taken at relatively low system pressures (0.13–0.19 MPa), and three inlet mass fluxes (G_1) were tested. In particular, low ($\sim$1350 kg/m^2 s), medium ($\sim$2050 kg/m^2 s), and high mass fluxes ($\sim$2700 kg/m^2 s) were investigated. Three inlet qualities (x_1) were investigated for each mass flux; 0.2, 0.3 and 0.4%. These conditions resulted in bubbly and bubbly–stratified flow regimes at the inlet (side 1). The mass extraction ratio (W_3/W_1) was varied over a wide range (from $\sim$0.02 to $\sim$0.95).

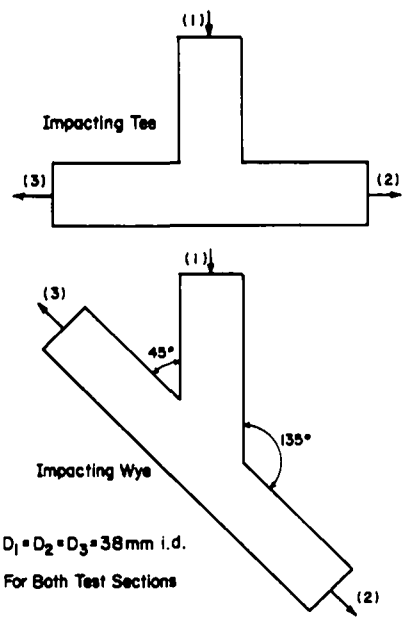

Figure 2. Test section configurations

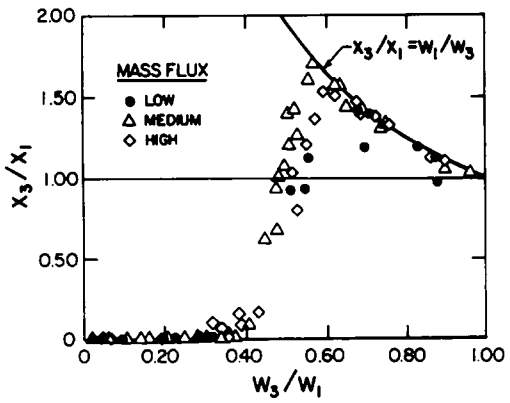

Figure 3. Phase separation data for the impacting tee.

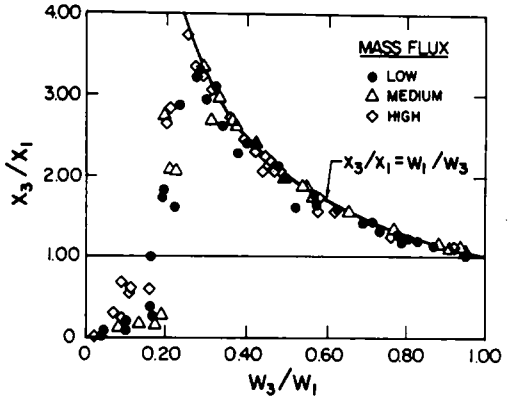

Figure 4. Phase separation data for the impacting wye.

A summary of the impacting tee data is shown in figure 3. It can be seen that up to a certain extraction ratio ($W_3/W_1 = 0.4$), very little of the gas phase is diverted to outlet side 3. At $W_3/W_1 = 0.5$ we find, as expected, $x_3 = x_2 = x_1$. Finally, for $W_3/W_1 > 0.6$, essentially conplete phase separation occurred (i.e. $x_3/x_1 = W_1/W_3$). Thus, it appears that an impacting tee behaves very much like a fluidic switch.

In contrast to the tee, the condition of equal phase distribution for the 45° wye occurred at $W_3/W_1 = 0.15$. Moreover, as can be seen in figure 4, at about $W_3/W_1 = 0.25$ nearly complete phase separation was observed (i.e. $x_3/x_1 = W_1/W_3$). These data trends are completely explainable in terms of the inertia of each phase (Hwang 1986). Briefly, the relatively large inertia of the liquid phase makes it more difficult for the liquid to change its direction of motion in order to exit through side 3. In contrast, the gas can more easily change direction.

Comparing figures 3 and 4 it can be noted that the impacting wye data show a significantly higher peak in x_3/x_1 than the impacting tee data and that the location of the peak is shifted to a lower W_3/W_1 than for the impacting tee. Again, this is a consequence of the relatively greater inertia of the liquid phase.

3. ANALYSIS

As discussed in the introduction, five independent equations are needed to solve for the five unknown state variables. Four of these equations can be easily determined from mass and momentum balances following an approach similar to the one outlined by Saba & Lahey (1984). Attention is focused here on the development of the "fifth equation" with which the phase separation for a given extraction rate can be determined.

3.1. The condition of equal phase separation

Figures 3 and 4 show that x_1, x_2 and x_3 are generally quite different, except for one particular extraction rate ($W_3/W_1 = 0.5$ for the impacting tee and $W_3/W_1 = 0.15$ for the 45° impacting wye) where equal phase separation (i.e. $x_1 = x_2 = x_3$) prevails. The objective here is to develop a simple theoretical basis for this condition. A derivation is performed for impacting wyes of any angle θ, keeping in mind that impacting tees correspond to the special case $\theta = 90°$.

Referring to figure 5, measurements of the pressure distribution around the junction performed in the present investigation suggest that the condition of equal phase separation coincides with equal pressure drops, $\Delta p_{12_j} = \Delta p_{13_j}$ (or $p_{2_j} = p_{3_j}$). For this condition there is no net pressure gradient in the z-direction at the junction. The existence of a pressure difference ($p_{2_j} - p_{3_j}$) will influence the two phases differently due to the differences in the inertia of each phase. Indeed, our measurements indicate that $x_3/x_1 < 1$ for $p_{2_j} < p_{3_j}$ and $x_3/x_1 > 1$ for $p_{2_j} > p_{3_j}$.

Based on the above discussion, the momentum balance for the control volume in figure 5 at the point of equal phase distribution can be approximated by

Rate of momentum outflow from the control volume in the z-direction

= Rate of momentum inflow into the control volume in the z-direction.

Thus,

$$W_3 u_3 - W_2 u_2 = -W_1 u_1 \cos\theta \quad [1]$$

where u_1, u_2 and u_3 are the mean velocities in sides 1, 2 and 3 of the junction, respectively. It should be noted that [1] is based on the fact that the pressure at side 1, p_{1_j}, has no force component in the z-direction, the pressures at sides 2 and 3 are assumed equal at the condition of even phase distribution and the z-component of the impacting force at the pipe wall is considered negligible. Further, [1] can be rewritten as

$$\frac{W_3^2}{\rho_3 A_3} - \frac{W_2^2}{\rho_2 A_2} + \frac{W_1^2 \cos\theta}{\rho_1 A_1} = 0, \quad [2]$$

where A_1, A_2 and A_3 are the areas of sides 1, 2 and 3, respectively, and ρ_1, ρ_2 and ρ_3 are the flow densities in sides 1, 2 and 3, respectively. Given that $x_1 = x_2 = x_3$, and assuming that the flow in the region of the junction is locally homogeneous (i.e. $\rho_1 = \rho_2 = \rho_3$), [2] yields

$$\frac{A_1}{A_3}\left(\frac{W_3}{W_1}\right)^2 - \frac{A_1}{A_2}\left(1 - \frac{W_3}{W_1}\right)^2 + \cos\theta = 0. \quad [3]$$

If $A_2 = A_3$ (the situation in our experiment and in most applications), [3] reduces to

$$\frac{W_3}{W_1} = \frac{\left(1 - \frac{A_3}{A_1}\cos\theta\right)}{2}. \quad [4]$$

Equation [4] is presumably valid for $0 < \theta < 180°$, and is based on an assumed $p_{2_j} = p_{3_j}$. In our experiment, $A_1 = A_2 = A_3$, thus, [4] yields for the flow split at equal phase distribution, $W_3/W_1 = 0.146$ for $\theta = 45°$, $W_3/W_1 = 0.5$ for $\theta = 90°$ and $W_3/W_1 = 0.854$ for $\theta = 135°$. These predictions (for $\theta = 45°$ and 90°) are in close agreement with the experimental results shown in figures 3 and 4.

3.2. *Unequal phase separation*

The flow situation in the junction is very complicated, however, a simplified approach is proposed here based on a balance between the dominant forces acting on each phase. This analysis is for the general case where $p_{2_j} \neq p_{3_j}$ (i.e. uneven phase separation) in a wye or a tee. The approach is based on the concept of "dividing streamlines", which was applied successfully to dividing junctions (Hwang *et al.* 1988).

Incoming liquid and gas flowing through side 1 of the junction may have to follow curved paths in order to exit through sides 2 or 3. For certain incoming flow regimes (e.g. bubble flow), the gas and liquid "streamlines" would have to cross if the phases were unevenly distributed among the two outlet branches. Figure 6 shows the dominant forces acting on the gas and liquid for typical streamlines crossing with an angle β. The gas and liquid velocities along these streamlines are u_G

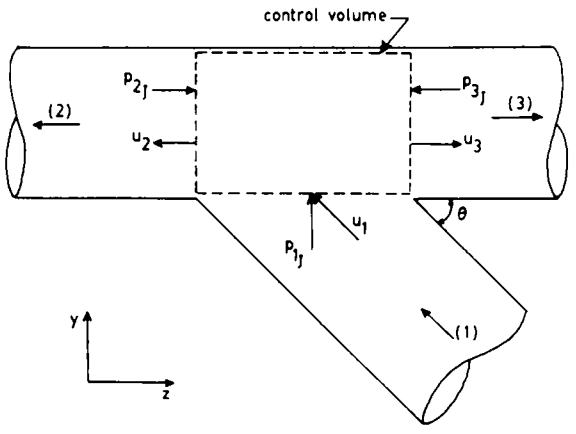

Figure 5. Flow parameters for an impacting wye.

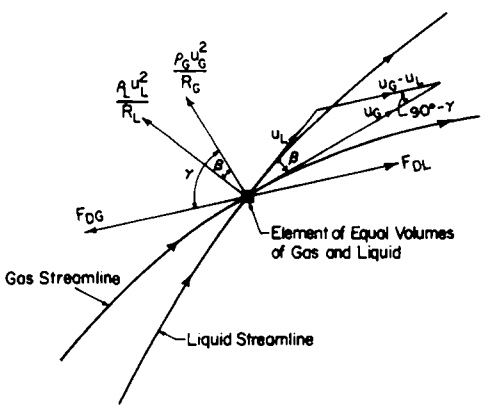

Figure 6. Balance of forces at a streamline crossing.

and u_L, respectively. Due to phasic slip, a volumetric drag force, F_{DF}, acts on the gas and an equal and opposite volumetric drag force, F_{DL}, acts on the liquid. Both drag forces act in a direction parallel to the relative velocity vector. Due to the motion along curved streamlines, the centrifugal forces per unit volume, $\rho_G u_G^2/R_G$ and $\rho_L u_L^2/R_L$, act on the gas and liquid, respectively, in directions normal to their streamlines, as shown in figure 6, where ρ_G and ρ_L are the gas and liquid densities, respectively, and R_G and R_L are the radii of curvature for the gas and liquid streamlines, respectively.

Considering a fluid element containing equal volumes of gas and liquid at a streamline crossing (as shown in figure 6) and applying Euler's s and n equations to the gas phase within the fluid element yields, respectively,

$$\frac{\partial p}{\partial s_G} = -F_{DG}\sin\gamma - \rho_G u_G \frac{\partial u_G}{\partial s_G} \qquad [5]$$

and

$$\frac{\partial p}{\partial n_G} = F_{DG}\cos\gamma + \rho_G \frac{u_G^2}{R_G}, \qquad [6]$$

where p is the pressure, s_G and n_G are the directions tangential and normal to the gas streamline, respectively, and γ is the angle in the velocity triangle of figure 6. All the terms in [5] and [6] respresent forces acting on the gas component within the fluid element per unit volume of gas. Similarly for the liquid phase,

$$\frac{\partial p}{\partial s_L} = F_{DL}\sin(\gamma-\beta) - \rho_L u_L \frac{\partial u_L}{\partial s_L} \qquad [7]$$

and

$$\frac{\partial p}{\partial n_L} = -F_{DL}\cos(\gamma-\beta) + \rho_L \frac{u_L^2}{R_L}, \qquad [8]$$

where s_L and n_L are the directions tangential and normal to the liquid streamline, respectively. Also, all the terms in [7] and [8] represent forces acting on the liquid component within the fluid element per unit volume of liquid.

Dynamic equilibrium exists when the resultant volumetric force (F_{NET}) acts equally on the gas and liquid fractions of the fluid element. This condition is shown graphically in figure 7 in which, for simplicity, we have neglected spatial accelerations, and the individual forces in [5]–[8] are identified. Denoting $F_D \triangleq |F_{DG}| = |F_{DL}|$, the equilibrium condition illustrated in figure 7 can be written as:

$$2F_D\sin\gamma = \frac{\rho_L u_L^2}{R_L}\sin\beta \qquad [9]$$

and

$$2F_D\cos\gamma = \frac{\rho_L u_L^2}{R_L}\cos\beta - \frac{\rho_G u_G^2}{R_G}. \qquad [10]$$

Dividing [9] by [10] we obtain

$$\tan\gamma = \frac{\sin\beta}{\left[\cos\beta - \left(\frac{\rho_G}{\rho_L}\right)\left(\frac{u_G}{u_L}\right)^2\left(\frac{R_L}{R_G}\right)\right]}. \qquad [11]$$

Also, a relationship for the slip ratio (S) can be derived by applying the so-called Sine Rule to the velocity triangle in figure 6, resulting in

$$S \triangleq \frac{u_G}{u_L} = \frac{\cos(\gamma-\beta)}{\cos\gamma}. \qquad [12]$$

For given values of the slip and density ratios, [11] and [12] provide very simply relations for the evaluation of angles β and γ provided that the shape of the streamlines is known. Next we consider these shapes.

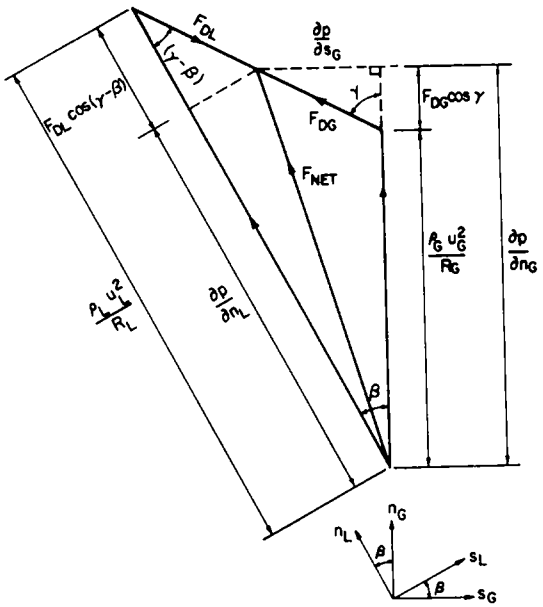

Figure 7. Force vector diagram.

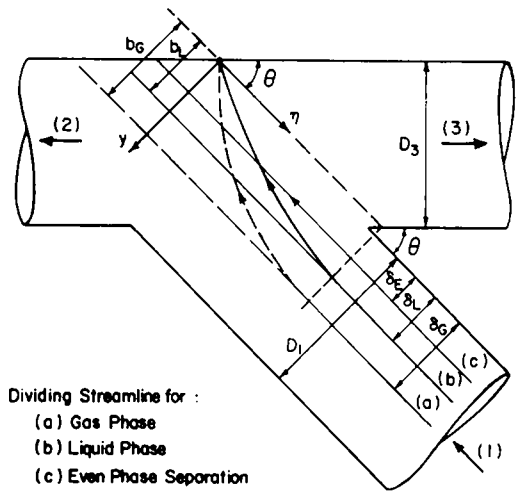

Figure 8. Dividing streamlines in an impacting wye.

3.3. *Dividing streamlines*

Our approach is based on the proposition that a "zone of influence" exists for each phase and that each "zone of influence" is bounded by a dividing streamline, as shown in figure 8. All liquid entering side 1 of the junction on the r.h.s. of the liquid dividing streamline (line b in figure 8) will exit through side 3 of the junction and the remaining liquid will exit through side 2. The gas phase behaves in a similar fashion with its split among sides 2 and 3 defined by the gas dividing streamline (line a in figure 8). The two dividing streamlines intersect at the point of impact with an angle β. Within the inlet branch, the gas and liquid dividing streamlines are assumed to be straight and separated by distances δ_G and δ_L from the conduit wall, respectively. However, as the junction region is approached, the dividing streamlines follow curved paths due to the pressure difference $(p_{2_j} - p_{3_j})$. For the condition of even phase distribution, characterized earlier by $p_{2_j} = p_{3_j}$, the dividing streamlines are assumed coincident and they remain straight (line c in figure 8) until the point of impact. The dividing streamlines at even phase distribution are separated by a distance δ_E from the conduit wall.

The shape of the dividing streamlines is not easy to determine in an exact manner. Nevertheless, an approximation can be made which satisfies all essential features. Our model is developed here for the general case of an impacting wye with arbitrary angle θ, keeping in mind that impacting tees correspond to the special case $\theta = 90°$. Using y–η coordinate system shown in figure 8, in which the origin is located at the point of impact, we assume the following form for the dividing streamlines:

$$\frac{y}{b_k} = 1 - \left(1 - \frac{\eta \sin\theta}{D_3}\right)^{m_k}, \quad \text{where } k = \text{G or L}. \tag{13}$$

The distance b_k (k = G or L) and the diameter D_3 are defined in figure 8 while the exponent m_k will be determined later. For even phase distribution, $m_k = 1$ and $b_k = 0$, the dividing streamlines are given by the straight line $y = 0$. For an uneven phase distribution ($b_k > 0$), the data indicate that $1 \leqslant m_k \leqslant 2$. Equation [13] has the following characteristics:

$$y = b_k, \quad \text{at } \eta = \frac{D_3}{\sin\beta}; \tag{14}$$

$$\frac{dy}{d\eta} = \frac{b_k}{D_1}\frac{D_1}{D_3} m_k \sin\theta, \quad \text{at } \eta = 0; \tag{15}$$

$$\frac{dy}{d\eta} = 0, \quad \text{at } \eta = \frac{D_3}{\sin\theta}; \tag{16}$$

$$\frac{d^2y}{d\eta^2} = -m_k(m_k - 1)\frac{b_k}{D_1}\frac{D_1}{D_3}\frac{1}{D_3}\sin^2\theta, \quad \text{at } \eta = 0. \tag{17}$$

Hence, from [15] and [17] we can formulate the radius of curvature of the dividing streamline of phase k at the point of impact ($\eta = 0$) as

$$\frac{R_k}{D_3} = \frac{\left[1 + \left(m_k \frac{D_1}{D_3}\frac{b_k}{D_1}\sin\theta\right)^2\right]^{3/2}}{m_k(m_k - 1)\frac{D_1}{D_3}\frac{b_k}{D_1}\sin^2\theta}; \tag{18}$$

and from [15], the angle β between the gas and liquid streamlines at the point of impact is given by

$$\beta = \tan^{-1}\left(m_G \frac{D_1}{D_3}\frac{b_G}{D_1}\sin\theta\right) - \tan^{-1}\left(m_L \frac{D_1}{D_3}\frac{b_L}{D_1}\sin\theta\right). \tag{19}$$

It should be noted that for a given junction geometry (i.e. specific D_3/D_1 and θ) and given values of the density ratio (ρ_G/ρ_L), slip ratio (S) and b_G/D_1, [11], [12], [18] and [19] provide the necessary relations for evaluating the corresponding b_L/D_1 if m_k is known. However, an iterative procedure is necessary due to the nonlinearity of these algebraic equations. In order to complete the development of our model the relationship between b_k/D_1 and W_{3k}/W_{1k} needs to be determined, as well as the functional relationship between m_k and the other parameters.

For the evaluation of W_{3L}/W_{1L} and W_{3G}/W_{1G}, we need to relate b_k and δ_k, defined in figure 8. We can use the properties that b_L/D_1 should go to unity when δ_L/D_1 becomes unity and b_L/D_1 must go to zero when δ_L/D_1 is equal to δ_E/D_1. A convenient function which has these properties is

$$\frac{b_L}{D_1} = \frac{\left(\frac{\delta_L}{D_1} - \frac{\delta_E}{D_1}\right)}{\left(1 - \frac{\delta_E}{D_1}\right)}. \tag{20}$$

From figure 8, we note that b_G can be related to b_L, δ_L and δ_G by

$$b_G = b_L + (\delta_G - \delta_L) \tag{21}$$

or

$$\frac{b_G}{D_1} = \frac{b_L}{D_1} + \left(\frac{\delta_G}{D_1} - \frac{\delta_L}{D_1}\right). \tag{22}$$

For an even phase distribution the ratios (W_{3k}/W_{1k}) and (W_3/W_1) are equal and they are both determined by [4] for given A_3/A_1 and θ. Knowing the extraction ratio at an even phase distribution, $(W_3/W_1)_E$, and assuming a uniform mass flux distribution for both phases, the angle ϕ in figure 9 can be easily determined from geometrical consideration as

$$\left(\frac{W_3}{W_1}\right)_E = \frac{[\phi - \frac{1}{2}\sin(2\phi)]}{\pi} \tag{23}$$

and the depth of the "zone of influence", given by

$$\frac{\delta_E}{D_1} = \frac{(1 - \cos\phi)}{2}. \tag{24}$$

For example, for impacting tees ($\theta = 90°$), we get $(W_3/W_1)_E = 0.5$, $\phi = 90°$ and $\delta_E/D_1 = 0.5$.

It was proposed earlier that for equal phase separation ($b_k = 0$) the dividing streamlines are straight ($m_k = 1$) and that their shape approaches that of a parabola ($m_k = 2$) as b_k/D_1 approaches

unity. Hence, from [18] we get the following formulation for the minimum radius of curvature at $b_k/D_1 = 1$:

$$\left(\frac{R_k}{D_3}\right)_{\min} = \frac{\left[1 + \left(2\frac{D_1}{D_3}\sin\theta\right)^2\right]^{3.2}}{2\left(\frac{D_1}{D_3}\right)\sin^2\theta}. \quad [25]$$

The radius of curvature varies from infinity at $b_k = 0$ down to the minimum value given by [25] at $b_k/D_1 = 1$. For simplicity, it was assumed that between these two extremes, the radius of curvature can be approximated by

$$\frac{R_k}{D_3} = \frac{\left(\frac{R_k}{D_3}\right)_{\min}}{\left(\frac{b_k}{D_1}\right)^{n_k}}. \quad [26]$$

The exponent n_k was determined empirically by comparing the analytical predictions of our model with the present phase separation data for the impacting tee and 45° wye. The best agreement was obtained with the following correlation:

$$n_k = 5 + 20\exp\left[-53\left(\frac{\delta_k}{D_1}\right)\right]. \quad [27]$$

Let us now summarize the computational procedure to be used in the evaluation of this model.

3.4. *Computational procedure*

The model presented above requires the following information as input data:

(1) The junction geometry given by D_1, D_2, D_3 and θ.
(2) The slip ratio (S) and density ratio ρ_G/ρ_L.
(3) The inlet flow regime and the corresponding mass distribution of both phases on the inlet side of the junction (in side 1).

With the specification of the above information, our model can be used to calculate W_{3G}/W_{1G} for any given W_{3L}/W_{1L} following these computational procedures:

(1) Calculate $(W_3/W_1)_E$ from [4] and δ_E/D_1 from [23] and [24].
(2) Calculate δ_L/D_1 from the given W_{3L}/W_{1L} and the given mass distributions of the liquid phase in side 1. A detailed discussion of this step with the associated area integrals for different inlet flow regimes has been given by Hwang (1986).
(3) Calculate n_L using [27] and b_L/D_1 from [20].
(4) Calculate $(R_L/D_3)_{\min}$ from [25]. Solve [18] and [26] iteratively for m_L.
(5) Assume a value for δ_G/D_1 and calculate b_G/D_1 from [22], n_G from [27], $(R_G/D_3)_{\min}$ from [25] and m_G from [18] and [26].
(6) Calculate β from [19], γ from [11] and S from [12].
(7) Compare S calculated from step (6) with the given value in the input data. If agreement within acceptable tolerance is not achieved, the assumed δ_G/D_1 in step (5) should be modified and steps (5)–(7) repeated until convergence is achieved.
(8) From the converged value of δ_G/D_1 and knowledge of the mass distribution of the gas phase in side 1, it is possible to compute W_{3G}/W_{1G}, since the "zone of influence" is specified by δ_G/D_1.

It must be noted that the slip ratio used in the above procedure should be taken as the mean value for the inlet mixture in side 1 since the model ignores the spatial acceleration of the phases in the junction region. The value of S in side 1 can be determined using drift–flux models or from a knowledge of the inlet flow regime and the corresponding mass distribution of both phases.

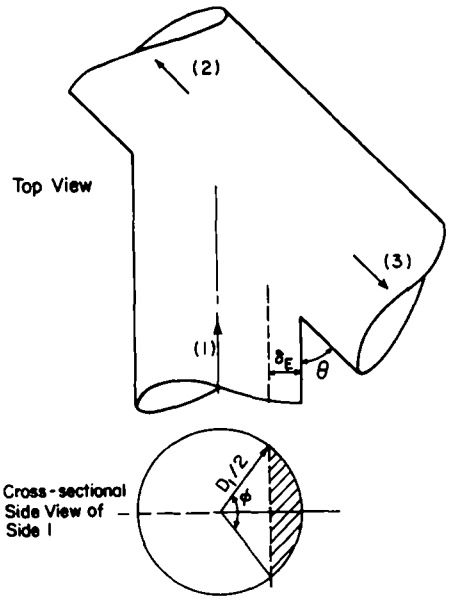

Figure 9. The "zone of influence" in an impacting wye.

Finally, values of W_3/W_1 and x_3/x_1 can be easily determined from W_{3G}/W_{1G}, W_{3L}/W_{1L} and x_1 using the following relations:

$$\frac{W_3}{W_1} = x_1\left(\frac{W_{3G}}{W_{1G}}\right) + (1 - x_1)\frac{W_{3L}}{W_{1L}} \quad [28]$$

and

$$\frac{x_3}{x_1} = \frac{\left(\frac{W_{3G}}{W_{1G}}\right)}{\left(\frac{W_3}{W_1}\right)}. \quad [29]$$

4. RESULTS AND DISCUSSION

4.1. Parametric analysis

A parametric analysis of the trends predicted by the model presented herein was performed for horizontal impacting junctions with $D_1 = D_2 = D_3$ and stratified flow entering through side 1. The predictions are shown in figure 10. As can be seen, a fluidic-switch-like behavior, which was noted in the data, was predicted. When the angle (θ) between the inlet and the side branch is small, the peak of x_3/x_1 occurs at low W_3/W_1 and the peak value of x_3/x_1 is large. For $\theta = 90°$, we see that $x_3/x_1 = 1.0$ when $W_3/W_1 = 0.5$. However, the slope of the curve and the peak of x_3/x_1 are smaller compared with the case of $\theta = 90°$. As expected, the slope and the peak value of x_3/x_1 decrease further for $\theta > 90°$.

4.2. Comparison with experimental data

Comparisons between model predictions and the data taken at RPI on the impacting tee and 45° wye are shown in figures 11 and 12, respectively. All branches were horizontal with stratified flow in the inlet side. The agreement shown in figures 11 and 12 is quite satisfactory.

The model was also assessed against the data of Azzopardi *et al.* (1987), which was taken in a vertical tee having equal-sized branches with annular flow in the inlet branch. Keeping in mind that these data correspond to flow conditions quite different from those used in model development, we find the good agreement in figure 13 quite encouraging in terms of model assessment.

An overall evaluation of our phase separation model is shown in figure 14 using all available data [present data and those of Azzopardi *et al.* (1987)]. It can be seen that the model is capable

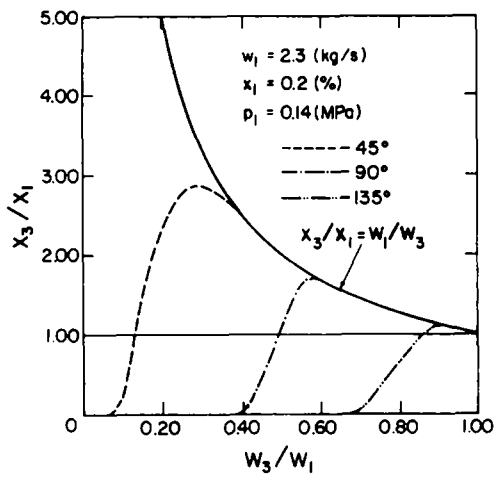

Figure 10. Phase separation for impacting air–water flows (horizontal, stratified flow regime). $W_1 = 2.3$ kg/s, $x_1 = 0.2\%$ and $p_1 = 0.14$ MPa.

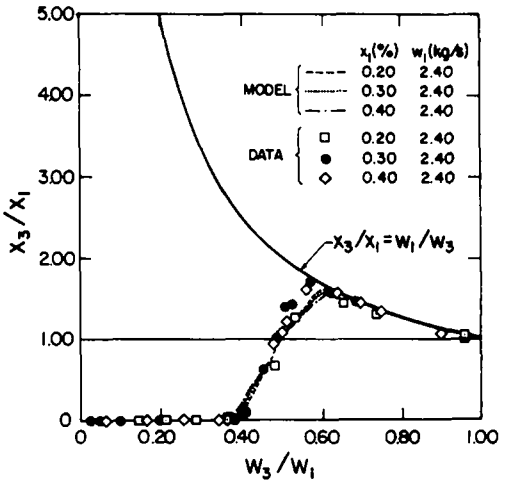

Figure 11. Comparison between present data and model predictions for an impacting tee.

of predicting more than 95% of the available data within $\pm 25\%$. The mean value of $(x_3/x_{1,\text{measured}})/(x_3/x_{1,\text{predicted}})$ is 0.99 with a standard deviation of 0.09. Moreover, the model predictions do not appear to be affected by flow regime or test section configuration (i.e. horizontal/vertical or wye/tee).

5. CONCLUSIONS

Phase separation experiments for impacting air–water two-phase flows in branching conduits were performed at RPI. Plexiglas wye and tee test sections were used in this study, thus allowing flow visualization. These test sections had branches of the same dimensions (i.e. $D_1 = D_2 = D_3 =$ 38 mm i.d.). The phase separation data showed that the peak in x_3/x_1 with respect to the mass extraction ratio (W_3/W_1) for the impacting tee case was lower than that for impacting wye cases in which the branch angle was $<90°$, and that the point where the peak occurred was at a lower mass extraction ratio. Moreover, it was observed that for impacting two-phase flows in a tee, an equal phase split (i.e. $x_3/x_1 = 1.0$) occurs when $W_3/W_1 = 0.5$. In contrast, for an impacting wye the values of W_3/W_1 at the point of equal phase split depends on the angle (θ) between the side branch and the inlet.

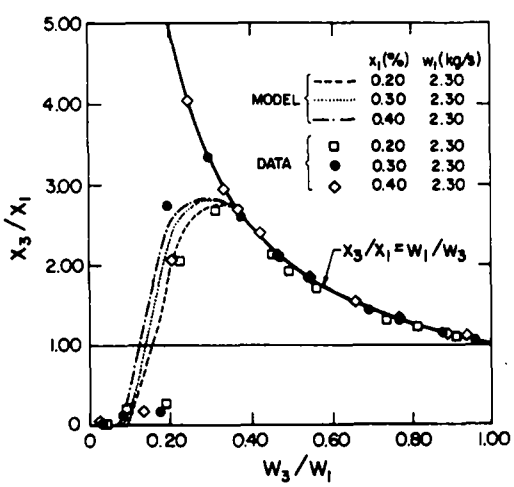

Figure 12. Comparison between present data and model predictions for an impacting 45° wye.

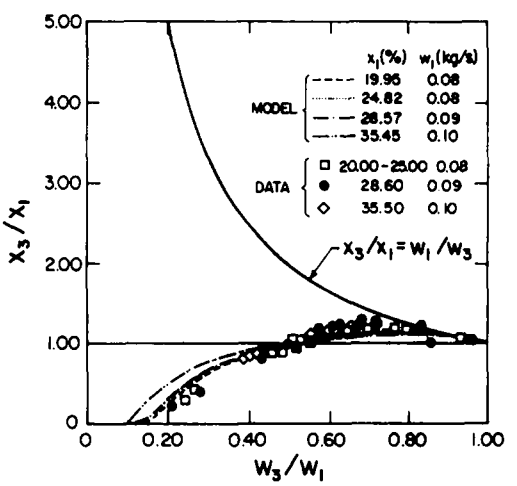

Figure 13. Comparison between the data of Azzopardi *et al.* (1987) and model predictions for an impacting tee.

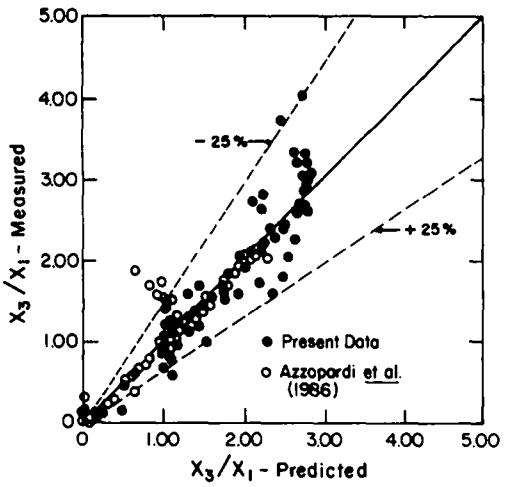

Figure 14. Prediction capabilities for all data of impacting two-phase flows.

Using a "dividing-streamline" approach an analytical model of phase separation for impacting two-phase flows in branching conduits was developed. This simple model was shown to predict the available data quite well. The analytical model presented herein should be useful for the analysis of phase separation in two-phase headers and the plena of heat exchangers and process equipment. It may also be applied to phase separation problems associated with the use of wet stream injection for enhanced petroleum recovery, and for the analysis of emergency core cooling during hypothetical nuclear reactor accidents.

Acknowledgements—This work was performed under the auspices of the National Science Foundation and the Natural Sciences and Engineering Research Council of Canada. Their support is gratefully acknowledged.

REFERENCES

AZZOPARDI, N. J., PURVIS, A. & GOVAN, A. H. 1987 Annular two-phase flow split at an impacting T. *Int. J. Multiphase Flow* **13**, 605–614.

HONG, K. C. 1978 Two-phase flow splitting at a pipe tee. *J. Petrol. Technol.* **30**, 290–296.

HWANG, S. T. 1986 A study on phase separation phenomena in branching conduits. Ph.D. Thesis, Rensselaer Polytechnic Inst., Troy, N.Y.

HWANG, S. T., SOLIMAN, H. M. & LAHEY, R. T. JR 1988 Phase separation in dividing two-phase flows. *Int. J. Multiphase Flow* **14**, 439–458.

SABA, N. & LAHEY, R. T. 1984 The analysis of phase separation phenomena in branching conduits. *Int. J. Multiphase Flow* **10**, 1–20.